

Water concentration profiles in natural mantle orthopyroxenes: A geochronometer for long annealing of xenoliths within magma

Zhen-Zhen Tian, Jia Liu*, Qun-Ke Xia, Jannick Ingrin, Yan-Tao Hao, Depecker

Christophe

SAMPLING AND THE HOSTING ROCKS

All the samples are from Dongfushan (DFS) volcano (32°35'41" N, 118°56'05" E) in the Tianchang County, Anhui Province, Eastern China, where large amount of center-eruptive Cenozoic volcanoes are distributed (Figure DR1A). So far, no publication has described volcanological and geochemical characteristics of Dongfushan volcano, and only sparse unpublished whole-rock major- and trace-elements data have been acquired (Dr. Zheng Xu in University of Science and Technology of China, personal communication). This volcano is small and isolated, with height less than 100 meters above the ground, which is similar to the Cenozoic center-type volcano nearby. A large open-pit crop (with diameter of 350 m) (Figure DR1B) dug in the volcano was explored during a field work on May 2013. Due to this artificial change, no clear volcanological structure (e.g. the position of the eruption center) could be identified. Abundant peridotite xenoliths appear in the lava flows from the shallow to the bottom. However, most of the xenoliths in the shallow depth are extensively altered (the olivines are nearly all serpentized). Thus, most of the samples in this study were collected from the bottom of this open-pit crop, which is about 10 meters below the surface of the lava flow (Figure DR1B).

The available geochemical data of the hosting rocks show that they are alkali basalts and have primitive mantle normalized trace element patterns similar to that of the others Cenozoic basalts in eastern China (OIB-like, enriched in large ion lithophile element (LILE) and light rare earth element (LREE), but not depleted in Nb and Ta) (e.g. Zou et al., 2000). The MgO contents of the bulk rocks vary from 7.14 to 12.37 wt.%, and the bulk rock Mg# ($\text{Mg\#} = \text{Mg}/(\text{Mg} + \text{Fe}) \times 100$ in mol., all Fe considered as Fe^{2+}) vary from 56 to 70. The (Nb/La)_n ratio (n represent primitive mantle normalization) are all around 1.6. Based on the correlation between liquidus temperature (T_{liquidus}) and Mg# of basaltic melts ($T_{\text{liquidus}}(^{\circ}\text{C}) = 1066 + 12.067\text{Mg\#} + 312.3(\text{Mg\#})^2$, Niu, 2005 and the references therein), the highest liquidus temperature of these Tianchang basalts is close to 1250°C. Compared with the temperature profiles in Alae lava lake (with total thickness of 15 m) measured over 4 years after its last eruption (Fig.3 and Fig. 10 in Peck, D. L. (1978); Cooling and vesiculation of Alae lava lake, Hawaii), we suggested that at about 10 meters below the surface of a lava flow with thickness of 15 m, the magma could definitely be cooled slowly, and stay at temperature near 850°C for a time period close to one year.

ANALYTICAL METRHODS

Fourier Transform Infrared Spectroscopy (FTIR)

FTIR measurements were conducted in the CAS Key Laboratory of Crust-Mantle Materials and Environments at the University of Science and Technology of China (CMME-USTC). Samples were prepared with two parallel polished surfaces. Mineral profiles in H₂O content were measured in transmission mode on a Spotlight 200 PerkinElmer FTIR spectrometer coupled with a PerkinElmer microscope using an OptKBr beam splitter and a liquid-nitrogen cooled MCT detector in a continuous dry nitrogen flush. A total of 64 scans for background and sample were

accumulated for each spectrum. The resolution was 4 cm^{-1} . Aperture size was set at $25\times 100\text{ }\mu\text{m}$, the shorter size along the measuring direction, with a spacing of 30 to $75\mu\text{m}$, depending on the mineral size.

The Omnic software was used to integrate the area beneath the OH bands. For the calculation of average water contents for each sample, a spline baseline correction was used. For the exploration of the potential H profile in cpx and opx, two kinds of baseline correction strategies (linear baseline and spline baseline) were tested, in the range from $3700\text{ to }2800\text{ cm}^{-1}$ for opx and $3700\text{ to }3000\text{ cm}^{-1}$ for cpx. The “internal” relative uncertainty of the two approaches is less than 5% (2SD). It was calculated from the dispersion of integral areas obtained with three different baselines. Usually, the spline approach lead to slightly larger integral area than the linear one. H_2O contents were calculated from a modified form of the Beer-Lambert law.

$$c=A / (\varepsilon \cdot t)$$

Where c is the content of hydrogen species (ppm H_2O by weight), A is 3 times the unpolarized integral absorption, ε is the integral specific absorption coefficient ($\text{ppm}^{-1}\text{ cm}^{-2}$) (Bell et al., 1995), t is the thickness (cm).

Electronic Back-Scattered Diffraction (EBSD)

The orientations of pyroxenes were determined by electron back-scattered diffraction (EBSD) in the China University of Geosciences (Wuhan) with a Quanta 450 scanning electron microscope. The measurements were carried out with an accelerating voltage of 20 kV, a spot size of $6.5\mu\text{m}$ and a working distance of 25 mm. Diffraction patterns were manually collected and indexed using the HKL Channel 5+ software to ensure data quality.

Compositional profile analysis by EPMA

Composition profiles were obtained with a Shimadzu Electron Probe Micro-analyzer (EPMA 1600) at CMME-USTC with operating conditions set as 15 kV for accelerating voltage, 20 nA for beam current and 1 μm for beam diameter. For opx, a routine single quantitative analysis mode was used to perform profile analysis. The standards are natural minerals and synthetic oxides, and a program based on the ZAF procedure was used for data correction. The measurements were made from the core to the rim of each mineral grain; and in general, three to four grains of each mineral phase were analyzed in each sample. The uncertainty for all elements was below 5%, except for Na, for which the uncertainty may be as high as 10%. For olivine, the “Linear composition analysis” mode was used, under which only the relative intensity (counts) of the element of interest was recorded.

Modeling details

3 dimensional diffusion modeling was performed to simulate water concentration profiles in the DFS opx grains. We considered the magma as an infinite sink for H. The initial water concentrations (C_i) was assumed to be the value of the plateau in the profile (e.g. the average concentration of all the data in the plateau). The water content in three-dimensions can then be described by the function $C(x,y,z,t)$ (Crank, 1956):

$$\frac{C(x,y,z,t) - C_0}{C_0 - C_1} = 1 - \frac{64}{\pi^3} \sum_{l=0}^{\infty} \sum_{m=0}^{\infty} \sum_{n=0}^{\infty} \frac{(-1)^{l+m+n}}{(2l+1)(2m+1)(2n+1)} \times \cos \frac{(2l+1)\pi x}{2a} \cos \frac{(2m+1)\pi y}{2b} \cos \frac{(2n+1)\pi z}{2c} \\ \times \exp \left[-\frac{\pi^2 t}{4} \left\{ \frac{D_x(2l+1)^2}{a^2} + \frac{D_y(2m+1)^2}{b^2} + \frac{D_z(2n+1)^2}{c^2} \right\} \right]$$

where $2a$, $2b$ and $2c$ are the lengths of the grain along x , y and z directions, C_0 is the initial water concentration; C_1 is the final concentration at the grain edge, and is assumed to be 20 ppm

for the two grains presented. D_x , D_y and D_z are the diffusion coefficients along x, y and z directions (they are assumed to be the same). For opx DFS16-opx7, $2a=2.05\text{mm}$ (profile along CD direction, Fig.2a), $2b=2.05\text{mm}$, and $2c=2.4\text{mm}$ (profile along RL direction, Fig. 2a); for opx DFS16-opx2, $2a=1.5\text{mm}$ (profile along CD direction, Fig. 2b), $2b=1.5\text{mm}$, $2c=3.825\text{mm}$ (profile along RL direction, Fig. 2b).

Supplementary figures

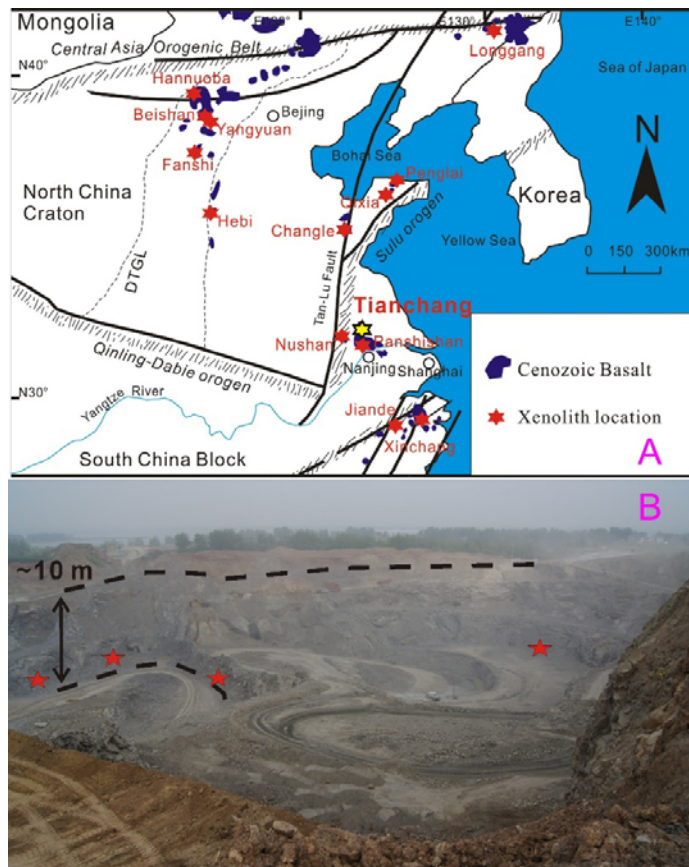


Figure DR1. A) Geographic location of the Tianchang volcanoes. Xenoliths hosted by the Cenozoic basalts in eastern China are also shown. DTGL: Daxing'anling-Taihangshan Gravity Lineament. B), Photo of the quarry in Tianchang volcano. The red stars mark the sampling locations.

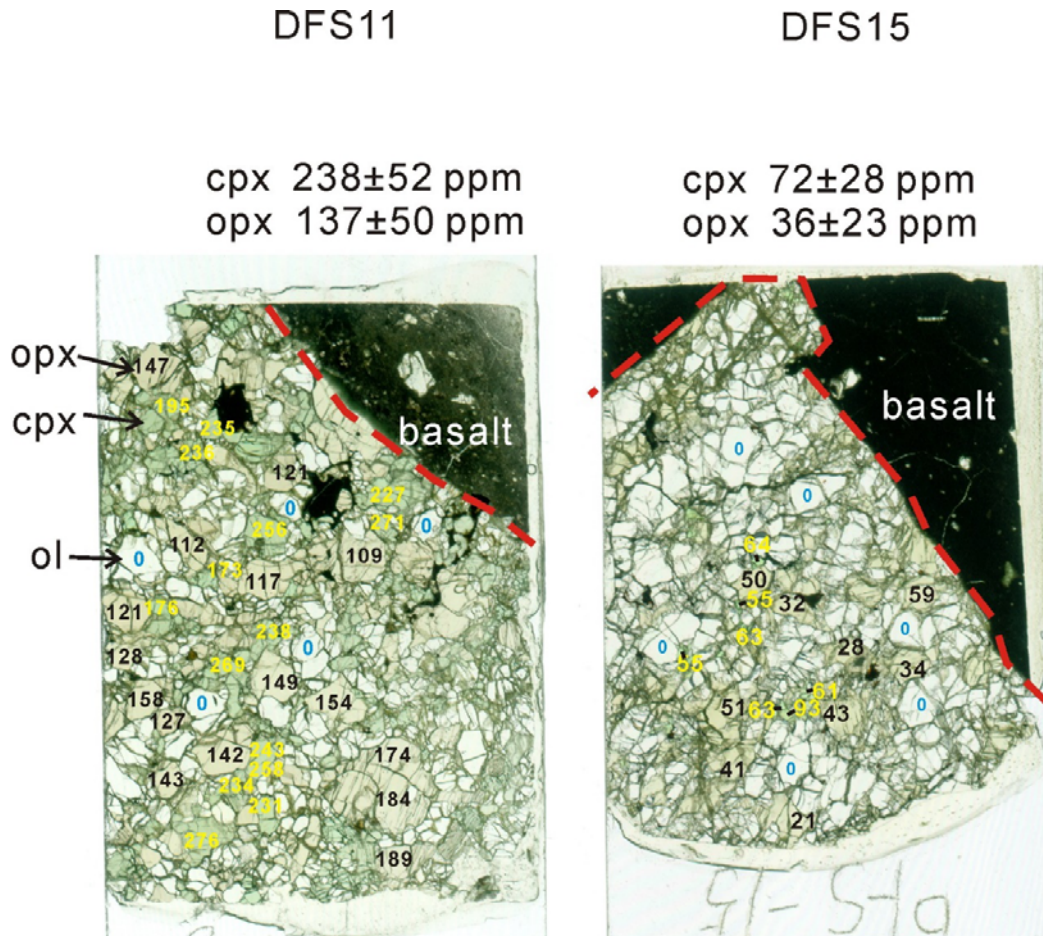


Figure DR2 Example of water concentration measurement in cpx, opx and olivine in Tianchang peridotite xenoliths. The width of each section is 2.5 cm. Photographs are scanned images of the thin sections with thickness around 200 μ m. The numbers marked on the images are the water content for the single grains that were calculated from the unpolarized FTIR analyses (3 times the unpolarized integral absorption). Black numbers for opx, yellow for cpx and blue for olivine. The average water contents of cpx and opx (with 2SD uncertainty) within one xenolith are also shown in the top. Xenolith DFS11 has comparable size with DFS15 in hand species, around 3~5 cm. Note that normally due to the anisotropy of spectra in pyroxenes, it make no sense to compare the water content for a single crystal, but here the distribution of these calculated water contents can statistically show that there is no significant difference for the pyroxenes in center and rim.

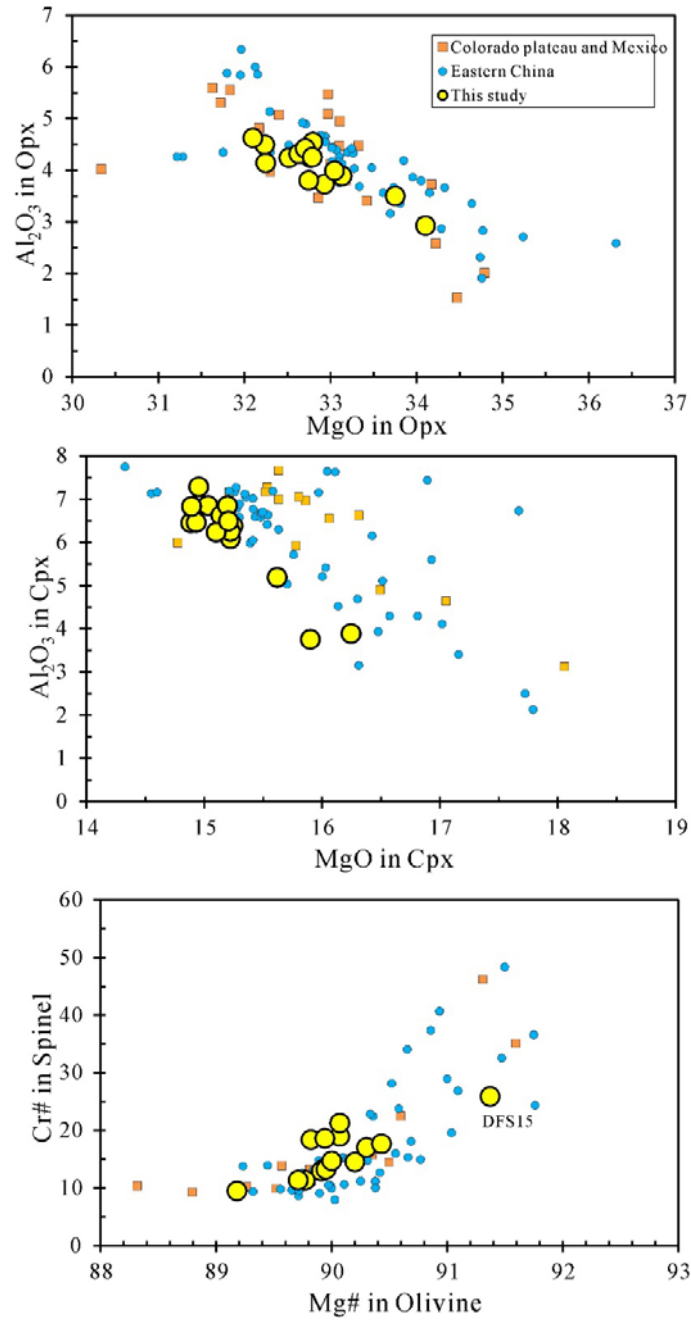


Figure DR3 Variation plots for major elements in opx, cpx and spinel. Al_2O_3 versus MgO in opx (a), in cpx (b) and Cr# in spinel versus Mg# in ol (c). Blue dots are data of peridotite xenoliths from the Subei basin (Panshishan, Lianshan and Fangshan, Bonadiman et al., 2009; Xia et al., 2010). Orange squares are the data of lherzilites from Colorado plateau and Mexico (Peslier, 2010). The large yellow dots are the data for the Tianchang xenoliths (Hao et al., (2016).

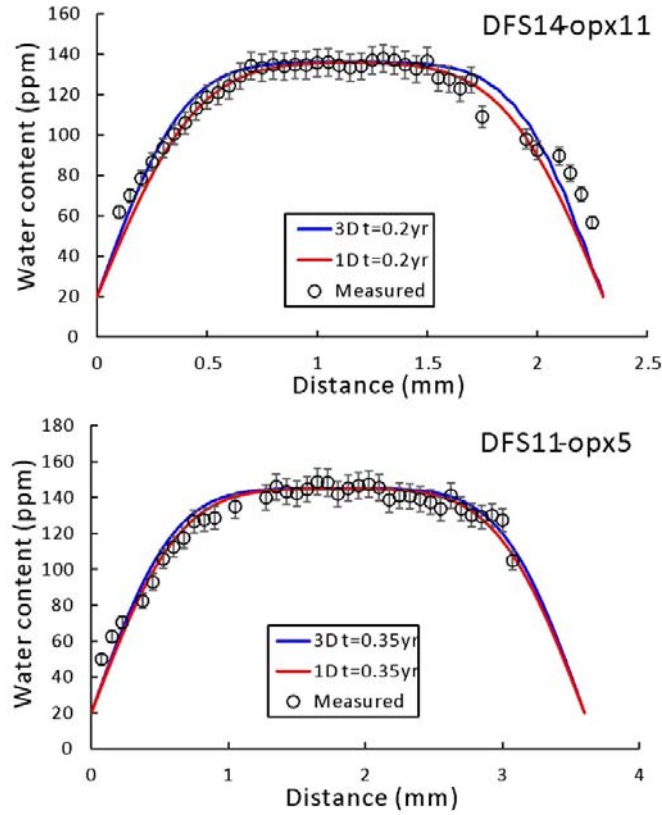


Figure DR4. Water concentration profiles in opx from the Tianchang peridotites. The simulation curves based on 1D and 3D diffusion models are shown for comparison. The 3D diffusion equation shown in section “Method” in this supplementary file was used. H diffusion in opx is considered to be isotropic, which is consistent with the experimental results (Stalder and Skogby, 2003, 2006; Sundvall et al., 2009a,b). Parameters are set as: for DFS14-opx11, $2a=2b=1.15\text{mm}$, $2c=2.3\text{mm}$, C_0 is 136 ppm, and C_i is 20 ppm; for DFS11-opx5, $2a=2b=2.73\text{mm}$, $2c=3.23\text{mm}$, C_0 is 146 ppm, and C_i is 20 ppm. $D_x=D_y=D_z=10^{-14}\text{m}^2/\text{s}$. The final water concentration of the rim (C_i) is set as 20 ppm. The open circles are the measured water contents. 1D model equation is

$$\frac{(C_x - C_0)}{(C_i - C_0)} = \text{erf}\left(\frac{x}{2\sqrt{Dt}}\right) + \text{erf}\left(\frac{L - x}{2\sqrt{Dt}}\right)$$

Where C_x is the water content at time t at distance x , L is the grain size (Crank, 1956). Other parameters are the same as in the 3D model equation. The data for the measured profile and modeling calculation are listed in Table DR6.

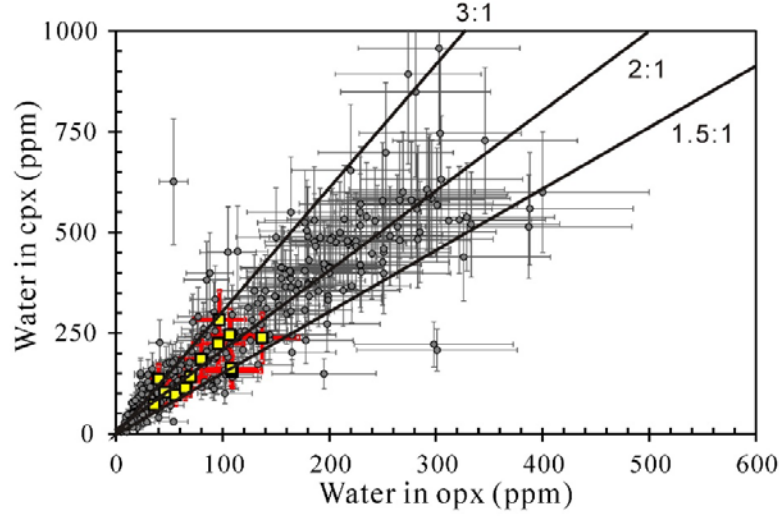


Figure DR5. Comparison of the average water contents in cpx and opx in Tianchang xenoliths with global data. The yellow squares show the water contents measured in the core of cpx and opx in this study, other data (gray dots) are from Demouchy and Bolfan-Casanova (2016). The water contents for Tianchang xenoliths are from Hao et al. (2016). Error bars (in red) are assumed to be 25% (2sd).

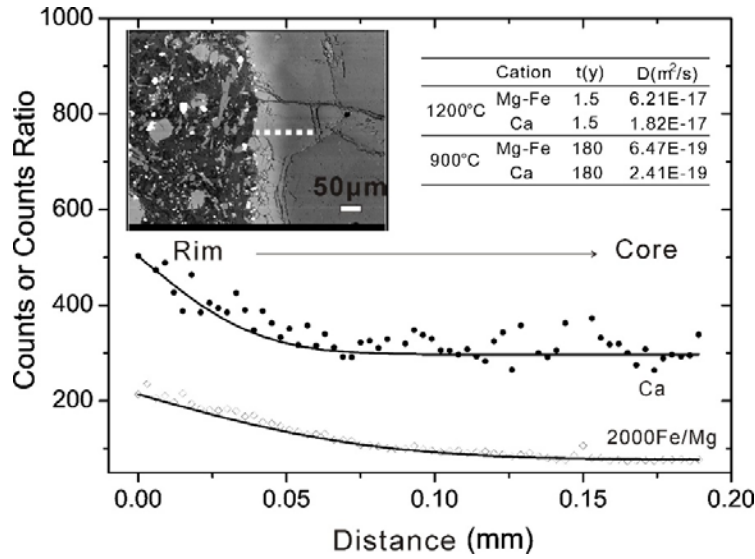


Figure DR6. Fe/Mg ratios and Ca concentration profiles measure on an olivine that was in contact with the host magma (DFS7-ol1). A one-dimensional composition-independent semi-infinite diffusion model was used to fit the measured data: $C(x, t) - C_0 = (C_1 - C_0) \operatorname{erfc} \frac{x}{2\sqrt{Dt}}$, where $C(x, t)$ is the concentration at a distance x from the interface between olivine and melt, $x=0$, after time, t , has elapsed; C_1 and C_0 are the concentrations of the diffusion species at the rim and the core,

respectively; D and t are diffusivity and time respectively. Black solid lines represent the result of fits. The diffusion coefficients for Fe-Mg and Ca in olivine are calculated from Dohmen and Chakraborty (2007) and Coogan et al. (2005), respectively. Model parameters: $T=1200^{\circ}\text{C}$, $X_{\text{Fe}}=0.172$, $f_{\text{O}_2}=\text{NNO-2}$, $P=50\text{MPa}$.

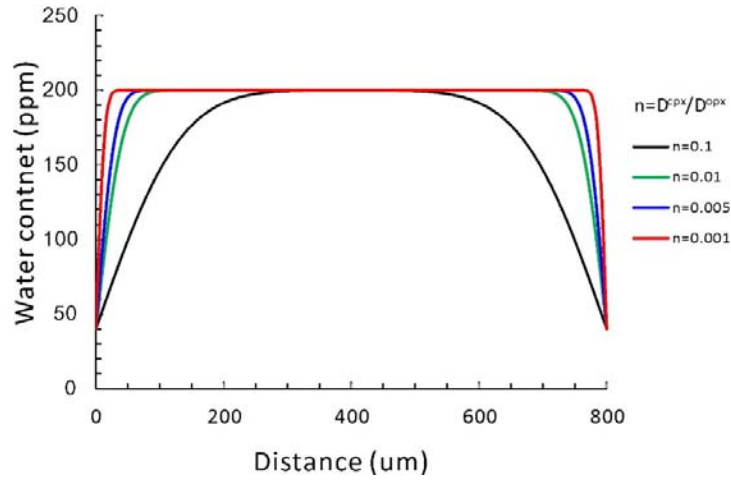


Figure DR7. 3D modeling of the H diffusion profile in cpx. The dimension of cpx is assumed to be: $2a=2b=0.8\text{mm}$, $2c=1.2\text{mm}$. H diffusion rate are 0.1, 0.01, 0.005, 0.001 times $10^{-14}\text{m}^2/\text{s}$ the one in opx (the same as in Figure DR7). C_i and C_1 are set at 200 and 40 ppm respectively. The diffusion time period is 0.2 year.

Table DR1 Major elements composition of cpx, opx and ol in Tianchang peridotites.

cpx	DFS1	1sd	DFS2	1sd	DFS3	1sd	DFS4	1sd	DFS5	1sd	DFS6	1sd	DFS7	1sd
Na ₂ O	1.63	0.14	1.63	0.02	1.50	0.07	1.80	0.05	1.49	0.05	1.61	0.03	1.16	0.11
K ₂ O	0.03	0.02	0.02	0.00	0.00	0.00	0.01	0.00	0.02	0.01	0.00	0.00	0.01	0.00
SiO ₂	52.36	0.47	52.85	0.37	52.88	0.04	53.01	0.30	52.69	0.32	52.25	0.16	52.32	0.36
Al ₂ O ₃	6.62	0.09	6.15	0.07	5.91	0.09	6.22	0.08	6.03	0.03	6.39	0.01	5.02	0.05
MgO	14.52	0.07	14.70	0.32	14.78	0.09	14.33	0.08	14.67	0.07	14.61	0.06	15.11	0.32
CaO	20.35	0.19	20.18	0.03	20.91	0.06	20.12	0.01	20.69	0.08	20.34	0.12	21.54	0.11
Cr ₂ O ₃	1.01	0.36	1.14	0.04	0.95	0.05	1.05	0.05	1.20	0.04	0.74	0.02	0.92	0.10
FeO	2.75	0.02	2.55	0.10	2.64	0.11	2.62	0.07	2.28	0.05	2.91	0.10	2.74	0.08
NiO	0.05	0.04	0.01	0.00	0.03	0.02	0.08	0.04	0.05	0.02	0.04	0.02	0.05	0.03
MnO	0.07	0.02	0.08	0.01	0.06	0.01	0.10	0.01	0.06	0.02	0.08	0.01	0.06	0.02
TiO ₂	0.40	0.26	0.36	0.03	0.38	0.04	0.39	0.05	0.32	0.02	0.40	0.04	0.26	0.02
Total	99.80		99.67		100.04		99.73		99.49		99.37		99.18	
opx	DFS1	1sd	DFS2	1sd	DFS3	1sd	DFS4	1sd	DFS5	1sd	DFS6	1sd	DFS7	1sd
Na ₂ O	0.12	0.02	0.10	0.03	0.08	0.01	0.10	0.02	0.08	0.02	0.08	0.02	0.06	0.02
K ₂ O	0.01	0.01	0.02	0.01	0.01	0.01	0.01	0.01	0.02	0.01	0.01	0.01	0.00	0.00
SiO ₂	55.70	0.72	55.84	0.32	55.60	0.35	55.81	0.22	55.66	0.50	55.07	0.19	55.67	0.48
Al ₂ O ₃	4.45	0.14	4.20	0.09	4.17	0.07	4.07	0.06	3.84	0.23	4.26	0.18	3.68	0.07
MgO	31.92	0.14	32.46	0.11	31.98	0.08	31.68	0.09	32.68	0.11	32.16	0.13	32.52	0.21
CaO	0.69	0.04	0.70	0.03	0.61	0.06	0.65	0.02	0.54	0.06	0.60	0.04	0.61	0.06
Cr ₂ O ₃	0.41	0.06	0.49	0.03	0.42	0.09	0.50	0.03	0.48	0.03	0.38	0.11	0.49	0.24
FeO	6.26	0.17	5.85	0.06	5.98	0.06	6.02	0.05	5.93	0.19	6.47	0.12	6.27	0.09
NiO	0.07	0.05	0.10	0.03	0.05	0.03	0.11	0.02	0.08	0.02	0.09	0.03	0.08	0.02
MnO	0.14	0.01	0.13	0.02	0.13	0.02	0.11	0.01	0.10	0.01	0.09	0.05	0.14	0.02
TiO ₂	0.20	0.10	0.12	0.01	0.09	0.02	0.09	0.02	0.07	0.01	0.08	0.01	0.06	0.02
Total	99.97		100.02		99.12		99.16		99.46		99.29		99.58	
ol	DFS1	1sd	DFS2	1sd	DFS3	1sd	DFS4	1sd	DFS5	1sd	DFS6	1sd	DFS7	1sd
SiO ₂	40.79	0.55	41.17	0.39	40.94	0.19	41.26	0.34	40.47	0.09	41.34	0.17	41.23	0.60
MgO	48.28	0.28	48.58	0.11	48.63	0.17	48.59	0.18	48.90	0.15	47.98	0.13	47.97	0.58
Al ₂ O ₃	0.03	0.01	0.02	0.01	0.00	0.00	0.01	0.01	0.01	0.00	0.01	0.01	0.00	0.00
CaO	0.06	0.01	0.06	0.01	0.05	0.01	0.05	0.01	0.02	0.00	0.05	0.01	0.03	0.01
FeO	9.80	0.12	9.31	0.09	9.42	0.08	9.17	0.21	9.62	0.12	9.81	0.11	9.69	0.15
Cr ₂ O ₃	0.22	0.27	0.02	0.02	0.04	0.02	0.03	0.01	0.01	0.02	0.08	0.08	0.03	0.02
MnO	0.11	0.02	0.09	0.01	0.11	0.02	0.08	0.04	0.08	0.02	0.09	0.02	0.12	0.02
TiO ₂	0.01	0.01	0.00	0.01	0.00	0.00	0.01	0.02	0.00	0.00	0.00	0.00	0.01	0.01
NiO	0.34	0.03	0.38	0.03	0.37	0.04	0.39	0.01	0.37	0.05	0.41	0.04	0.41	0.07
Total	99.64		99.63		99.57		99.60		99.47		99.76		99.49	

Note: Data for each sample are the average of four measurements, which were conducted on minerals randomly distributed in each section. 1sd is the standard deviation. All data are from Hao et al., (2016).

Table DR1 Major elements composition of cpx, opx and ol in Tianchang peridotites (continued)

cpx	DFS8	1sd	DFS9	1sd	DFS10	1sd	DFS11	1sd	DFS13	1sd	DFS14	1sd	DFS15	1sd	DFS16	1sd
Na ₂ O	1.54	0.01	1.31	0.11	1.64	0.02	0.11	0.11	1.59	0.03	1.57	0.06	0.79	0.02	1.62	0.09
K ₂ O	0.00	0.01	0.01	0.01	0.00	0.00	0.00	0.00	0.00	0.00	0.01	0.00	0.00	0.00	0.00	0.00
SiO ₂	52.21	0.36	54.42	0.35	52.65	0.36	0.60	0.60	52.97	0.50	52.78	0.33	53.30	0.40	53.31	0.27
Al ₂ O ₃	5.97	0.08	3.65	0.40	6.60	0.06	0.10	0.10	6.25	0.21	6.57	0.09	3.78	0.06	6.30	0.13
MgO	14.46	0.11	15.44	0.51	14.64	0.12	0.23	0.23	14.44	0.17	14.33	0.34	15.80	0.21	14.76	0.04
CaO	20.70	0.04	21.49	0.64	19.89	0.15	0.14	0.14	20.77	0.17	19.94	0.13	22.73	0.20	20.13	0.01
Cr ₂ O ₃	1.15	0.07	0.76	0.10	1.00	0.31	0.09	0.09	0.97	0.10	0.85	0.04	1.13	0.11	0.93	0.09
FeO	2.43	0.06	2.10	0.25	2.53	0.10	0.07	0.07	2.27	0.08	2.60	0.12	1.64	0.09	2.57	0.02
NiO	0.07	0.02	0.04	0.02	0.03	0.01	0.01	0.01	0.02	0.03	0.04	0.01	0.01	0.01	0.05	0.02
MnO	0.07	0.00	0.05	0.02	0.07	0.01	0.03	0.03	0.06	0.02	0.06	0.02	0.05	0.01	0.07	0.01
TiO ₂	0.35	0.02	0.07	0.01	0.41	0.06	0.02	0.02	0.40	0.01	0.43	0.07	0.05	0.03	0.35	0.04
Total	98.94		99.34		99.46		99.80		99.74		99.18		99.27		100.09	
opx	DFS8	1sd	DFS9	1sd	DFS10	1sd	DFS11	1sd	DFS13	1sd	DFS14	1sd	DFS15	1sd	DFS16	1sd
Na ₂ O	0.05	0.02	0.01	0.00	0.08	0.01	0.07	0.01	0.07	0.02	0.08	0.01	0.03	0.01	0.10	0.03
K ₂ O	0.01	0.01	0.00	0.00	0.01	0.01	0.00	0.00	0.00	0.00	0.00	0.00	0.01	0.00	0.01	0.01
SiO ₂	56.00	0.27	55.64	0.58	55.25	0.51	55.53	0.48	56.25	0.38	55.52	0.51	56.61	0.22	55.87	0.32
Al ₂ O ₃	3.76	0.12	3.47	0.14	4.48	0.13	4.57	0.06	3.96	0.11	4.36	0.09	2.89	0.23	4.21	0.05
MgO	32.35	0.62	33.50	0.14	32.35	0.41	31.73	0.25	32.79	0.11	32.25	0.20	33.65	0.23	32.49	0.14
CaO	0.60	0.08	0.58	0.06	0.61	0.01	0.62	0.02	0.55	0.05	0.61	0.02	0.45	0.02	0.68	0.07
Cr ₂ O ₃	0.43	0.06	0.37	0.04	0.35	0.04	0.26	0.06	0.32	0.08	0.50	0.15	0.60	0.15	0.41	0.09
FeO	6.08	0.11	6.06	0.10	5.95	0.09	6.40	0.13	5.67	0.25	5.87	0.09	5.08	0.22	5.84	0.05
NiO	0.09	0.02	0.05	0.02	0.07	0.03	0.07	0.03	0.08	0.06	0.11	0.03	0.07	0.03	0.06	0.05
MnO	0.12	0.03	0.12	0.02	0.12	0.02	0.11	0.01	0.12	0.02	0.11	0.03	0.10	0.01	0.09	0.02
TiO ₂	0.08	0.02	0.01	0.02	0.10	0.01	0.13	0.01	0.09	0.03	0.09	0.03	0.01	0.02	0.06	0.03
Total	99.56		99.81		99.36		99.50		99.90		99.51		99.51		99.83	
ol	DFS8	1sd	DFS9	1sd	DFS10	1sd	DFS11	1sd	DFS13	1sd	DFS14	1sd	DFS15	1sd	DFS16	1sd
SiO ₂	40.84	0.17	41.06	0.33	40.34	0.28	40.16	0.16	40.52	0.29	40.47	0.29	40.56	0.52	40.20	0.39
MgO	48.23	0.18	48.33	0.22	48.76	0.15	48.24	0.20	48.52	0.19	48.48	0.11	49.63	0.18	48.93	0.10
Al ₂ O ₃	0.02	0.02	0.00	0.00	0.02	0.01	0.01	0.01	0.01	0.01	0.01	0.01	0.01	0.00	0.02	0.01
CaO	0.04	0.01	0.03	0.01	0.04	0.01	0.04	0.01	0.03	0.00	0.06	0.02	0.05	0.03	0.06	0.01
FeO	9.61	0.17	9.50	0.37	9.74	0.10	10.43	0.21	9.71	0.09	9.66	0.18	8.40	0.34	9.69	0.06
Cr ₂ O ₃	0.03	0.03	0.07	0.08	0.00	0.01	0.04	0.03	0.02	0.02	0.25	0.34	0.30	0.34	0.03	0.02
MnO	0.12	0.04	0.14	0.03	0.10	0.03	0.10	0.02	0.10	0.02	0.12	0.01	0.10	0.02	0.11	0.01
TiO ₂	0.01	0.02	0.01	0.01	0.01	0.01	0.00	0.00	0.01	0.01	0.02	0.02	0.01	0.02	0.00	0.00
NiO	0.37	0.05	0.37	0.05	0.39	0.01	0.33	0.02	0.40	0.04	0.38	0.03	0.33	0.02	0.39	0.06
Total	99.26		99.52		99.40		99.34		99.30		99.44		99.39		99.42	

Note: 1sd is the standard deviation of four measurements. All data are from Hao et al., (2016).

Table DR2 Major elements composition along the traverse in the clinopyroxene DFS6-cpx3.

	rim										core										rim	Kunlun Di	Jaipur Di	PMR-53
(wt.%)	1-1	1-2	1-3	1-4	1-5	1-6	1-7	1-8	1-9	1-10	1-11	1-12	1-14	1-15	1-16	1-17	1-18	1-19	1-20					
SiO ₂	53.31	52.16	52.73	53.24	52.64	52.89	51.86	52.64	52.28	52.07	52.43	51.80	52.41	52.38	53.40	52.28	51.66	52.19	53.20	55.81	54.31	54.35		
Al ₂ O ₃	6.29	6.53	6.59	6.60	6.68	6.65	6.66	6.74	6.84	6.65	6.83	6.83	6.66	6.72	6.55	6.48	4.58	6.54	6.51	0.03	0.03	0.37		
TiO ₂	0.55	0.53	0.51	0.41	0.52	0.49	0.58	0.48	0.49	0.49	0.40	0.53	0.55	0.53	0.49	0.51	0.57	0.44	0.45	0.84	0.51	2.80		
Cr ₂ O ₃	0.72	1.73	0.68	0.80	0.67	0.81	1.05	0.86	0.68	0.92	0.86	0.98	0.88	0.84	0.86	0.86	0.74	0.57	0.68	0.01	0.01	0.17		
FeO	2.69	2.85	2.68	2.71	2.57	2.75	2.75	2.59	2.76	2.83	2.68	2.75	2.83	2.77	2.69	2.64	2.91	2.73	2.83	0.83	2.48	7.12		
NiO	0.06	0.01	0.00	0.06	0.04	0.03	0.06	0.00	0.02	0.02	0.05	0.01	0.02	0.10	0.03	0.04	0.05	0.06	0.05	0.01	0.01	0.07		
MnO	0.05	0.06	0.09	0.11	0.06	0.09	0.08	0.06	0.03	0.07	0.07	0.10	0.07	0.05	0.06	0.05	0.03	0.07	0.04	0.08	0.06	0.17		
MgO	15.16	14.64	14.11	14.84	15.01	14.62	14.41	14.40	15.23	14.37	14.85	14.53	14.89	14.98	14.73	13.89	16.19	14.34	15.17	17.99	17.09	18.23		
CaO	20.02	19.88	20.63	20.25	20.43	20.05	20.09	20.24	20.24	20.07	20.25	19.75	20.00	20.27	20.34	20.31	22.46	19.85	20.40	24.62	24.49	13.86		
Na ₂ O	1.59	1.46	1.65	1.61	1.69	1.67	1.64	1.70	1.46	1.68	1.64	1.61	1.74	1.66	1.60	1.67	0.50	1.64	1.60	0.57	0.38	2.03		
K ₂ O	0.00	0.03	0.00	0.02	0.02	0.01	0.00	0.01	0.01	0.01	0.00	0.01	0.02	0.00	0.00	0.00	0.02	0.00	0.00	0.01	0.01	0.04		
Total	100.43	99.88	99.66	100.64	100.32	100.04	99.19	99.72	100.04	99.18	100.05	98.89	100.07	100.31	100.76	98.73	99.72	98.42	100.93	100.84	99.39	99.24		
a.p.f.u																								
Si	1.911	1.888	1.909	1.907	1.893	1.906	1.890	1.903	1.886	1.897	1.892	1.890	1.892	1.887	1.910	1.911	1.886	1.911	1.902	1.995	1.984	1.974		
Ti	0.015	0.014	0.014	0.011	0.014	0.013	0.016	0.013	0.013	0.013	0.011	0.014	0.015	0.014	0.013	0.014	0.016	0.012	0.012	0.001	0.001	0.010		
Al	0.266	0.279	0.281	0.278	0.283	0.283	0.286	0.287	0.291	0.285	0.290	0.294	0.283	0.285	0.276	0.279	0.197	0.282	0.274	0.035	0.022	0.120		
Cr	0.021	0.050	0.020	0.023	0.019	0.023	0.030	0.025	0.019	0.026	0.024	0.028	0.025	0.024	0.024	0.025	0.021	0.016	0.019	0.000	0.000	0.005		
Fe	0.081	0.086	0.081	0.081	0.077	0.083	0.084	0.078	0.083	0.086	0.081	0.084	0.086	0.083	0.081	0.081	0.089	0.083	0.085	0.025	0.075	0.216		
Mn	0.002	0.002	0.003	0.003	0.002	0.003	0.002	0.002	0.001	0.002	0.002	0.003	0.002	0.001	0.002	0.001	0.001	0.002	0.001	0.002	0.002	0.005		
Mg	0.810	0.790	0.761	0.792	0.805	0.785	0.783	0.776	0.819	0.780	0.798	0.791	0.801	0.805	0.785	0.757	0.881	0.783	0.809	0.958	0.931	0.987		
Ca	0.769	0.771	0.800	0.777	0.787	0.774	0.784	0.784	0.782	0.783	0.783	0.772	0.773	0.783	0.779	0.795	0.879	0.778	0.781	0.943	0.958	0.539		
Na	0.110	0.103	0.116	0.112	0.118	0.117	0.116	0.119	0.102	0.118	0.115	0.114	0.122	0.116	0.111	0.118	0.036	0.116	0.111	0.040	0.027	0.143		
K	0.000	0.001	0.000	0.001	0.001	0.000	0.000	0.000	0.001	0.000	0.000	0.000	0.001	0.000	0.000	0.000	0.001	0.000	0.000					
Ni	0.002	0.000	0.000	0.002	0.001	0.001	0.002	0.000	0.001	0.001	0.001	0.000	0.000	0.003	0.001	0.001	0.002	0.002	0.001					
Total	3.986	3.985	3.985	3.987	4.001	3.987	3.994	3.988	3.997	3.993	3.998	3.991	4.000	4.002	3.982	3.982	4.007	3.986	3.995	4.000	4.000	4.000		
Mg#	90.96	90.15	90.39	90.72	91.24	90.47	90.32	90.85	90.78	90.07	90.82	90.42	90.36	90.60	90.70	90.37	90.83	90.37	90.53	97.5	92.5	82.0		

Note: Atomic concentration is calculated based on 6 oxygens in the pyroxene formula. $Mg\# = Mg/(Mg+Fe) \times 100$, all Fe is considered as Fe²⁺. The cpx grain are very homogenous in water as shown in Figure 2B. The data for diopside (Kunlun diopside and Jaipur diopside) and augite (PMR-53), which were frequently studied for H diffusion rate in the literature, are from Ferris et al. (2016).

Table DR3 Major elements composition along the traverse in orthopyroxene DFS16-opx7.

	rim										core										rim			
(wt.%)	1	2	3	4	5	6	7	8	9	10	11	12	13	14	15	16	17	18	19	20	21	22	23	24
SiO ₂	55.93	55.91	55.87	55.57	55.16	55.71	55.58	56.10	56.27	55.90	55.71	56.12	56.13	56.10	56.17	56.13	55.86	56.08	56.28	56.22	56.57	55.18	56.53	55.61
Al ₂ O ₃	4.17	4.30	4.31	4.30	4.26	4.18	4.34	4.26	4.44	4.41	4.43	4.28	4.38	4.27	4.45	4.35	4.17	4.31	4.19	4.26	4.36	4.38	4.40	4.44
TiO ₂	0.07	0.05	0.12	0.12	0.08	0.07	0.09	0.08	0.09	0.11	0.09	0.03	0.14	0.09	0.11	0.06	0.18	0.09	0.05	0.09	0.09	0.07	0.11	0.14
Cr ₂ O ₃	0.35	0.37	0.42	0.47	0.41	0.45	0.47	0.45	0.35	0.46	0.49	0.43	0.39	0.49	0.41	0.54	0.42	0.40	0.44	0.40	0.50	0.47	0.41	0.36
FeO	6.02	5.95	5.79	5.88	6.00	5.84	5.92	6.09	5.99	5.85	5.82	5.71	5.96	5.93	6.09	5.90	6.01	6.12	5.99	5.79	6.02	6.15	5.89	5.96
NiO	0.14	0.12	0.09	0.10	0.13	0.06	0.10	0.14	0.07	0.04	0.13	0.11	0.06	0.08	0.10	0.04	0.10	0.13	0.14	0.11	0.07	0.09	0.10	0.06
MnO	0.11	0.10	0.14	0.12	0.10	0.10	0.07	0.12	0.10	0.10	0.12	0.12	0.08	0.09	0.08	0.07	0.06	0.12	0.11	0.10	0.11	0.11	0.09	0.12
MgO	32.47	32.36	32.30	32.38	32.63	32.38	32.38	32.26	32.14	32.29	32.35	32.39	32.35	30.43	32.32	31.98	32.32	32.19	32.45	32.37	32.12	32.36	32.24	32.46
CaO	0.64	0.61	0.64	0.65	0.64	0.64	0.62	0.68	0.67	0.69	0.67	0.68	0.66	0.66	0.65	0.67	0.68	0.66	0.66	0.68	0.64	0.62	0.64	0.65
Na ₂ O	0.12	0.09	0.09	0.08	0.09	0.10	0.07	0.04	0.07	0.11	0.10	0.07	0.09	0.11	0.09	0.08	0.09	0.11	0.08	0.11	0.08	0.11	0.09	0.11
K ₂ O	0.00	0.00	0.00	0.00	0.00	0.00	0.00	0.00	0.01	0.00	0.00	0.02	0.01	0.00	0.00	0.00	0.00	0.01	0.00	0.01	0.00	0.00	0.00	0.00
Total	100.01	99.84	99.77	99.68	99.48	99.51	99.63	100.23	100.19	99.94	99.91	99.96	100.23	98.24	100.48	99.82	99.90	100.23	100.39	100.12	100.55	99.54	100.50	99.90
a.p.f.u																								
Si	1.926	1.927	1.927	1.920	1.912	1.927	1.921	1.928	1.932	1.924	1.920	1.931	1.927	1.960	1.925	1.934	1.926	1.928	1.930	1.931	1.935	1.913	1.934	1.917
Al	0.169	0.175	0.175	0.175	0.174	0.170	0.177	0.173	0.180	0.179	0.180	0.173	0.177	0.176	0.180	0.176	0.170	0.175	0.169	0.172	0.176	0.179	0.177	0.180
Ti	0.002	0.001	0.003	0.003	0.002	0.002	0.002	0.002	0.002	0.003	0.002	0.001	0.004	0.002	0.003	0.002	0.005	0.002	0.001	0.002	0.002	0.002	0.003	0.004
Cr	0.009	0.010	0.011	0.013	0.011	0.012	0.013	0.012	0.009	0.012	0.013	0.012	0.010	0.013	0.011	0.015	0.012	0.011	0.012	0.011	0.014	0.013	0.011	0.010
Fe	0.173	0.171	0.167	0.170	0.174	0.169	0.171	0.175	0.172	0.168	0.168	0.164	0.171	0.173	0.174	0.170	0.173	0.176	0.172	0.166	0.172	0.178	0.169	0.172
Ni	0.004	0.003	0.002	0.003	0.003	0.002	0.003	0.004	0.002	0.001	0.004	0.003	0.002	0.002	0.003	0.001	0.003	0.004	0.004	0.003	0.002	0.002	0.003	0.002
Mn	0.003	0.003	0.004	0.003	0.003	0.003	0.002	0.004	0.003	0.003	0.003	0.004	0.002	0.003	0.002	0.002	0.002	0.003	0.003	0.003	0.003	0.003	0.003	0.004
Mg	1.668	1.663	1.661	1.668	1.687	1.669	1.668	1.653	1.645	1.657	1.662	1.661	1.655	1.585	1.651	1.642	1.661	1.650	1.659	1.658	1.638	1.672	1.644	1.669
Ca	0.024	0.022	0.024	0.024	0.024	0.024	0.023	0.025	0.025	0.025	0.025	0.025	0.024	0.025	0.024	0.025	0.025	0.024	0.024	0.025	0.023	0.023	0.024	0.024
Na	0.008	0.006	0.006	0.005	0.006	0.007	0.005	0.003	0.005	0.007	0.006	0.005	0.006	0.007	0.006	0.005	0.006	0.007	0.006	0.007	0.005	0.008	0.006	0.007
K	0.000	0.000	0.000	0.000	0.000	0.000	0.000	0.000	0.000	0.000	0.000	0.001	0.000	0.000	0.000	0.000	0.000	0.001	0.000	0.001	0.000	0.000	0.000	0.000
Total	3.986	3.982	3.980	3.985	3.996	3.984	3.984	3.979	3.974	3.981	3.984	3.979	3.979	3.947	3.980	3.972	3.982	3.981	3.981	3.979	3.971	3.993	3.972	3.988
Mg#	90.58	90.66	90.87	90.75	90.65	90.82	90.70	90.42	90.54	90.78	90.83	91.01	90.63	90.15	90.45	90.62	90.55	90.36	90.62	90.88	90.48	90.37	90.70	90.67

Note: Atomic concentration is calculated based on 6 oxygens in the pyroxene formula. $Mg\# = Mg/(Mg+Fe) \times 100$, all Fe is considered as Fe²⁺.

Table DR4 Water concentration in cpxs, the core of opx, selected chemical indices and estimated equilibrium temperatures of the Tianchang peridotites.

Sample	H ₂ O (ppm)		Mg [#]			(La/Yb) _n ^{cpx}	T _{cpx-opx}	T _{Cao-opx}
	cpx	opx	ol	cpx	opx			
DFS1	246(15)	107(15)	89.77	90.39	90.09	0.35	978	965
DFS2	185(16)	80(15)	90.30	91.15	90.81	2.13	1004	967
DFS3	223(15)	96(19)	90.20	90.90	90.50	0.16	945	939
DFS4	283(16)	97(16)	90.43	90.69	90.36	4.20	978	954
DFS5	135(11)	40(16)	90.07	91.98	90.77	0.51	962	911
DFS6	222(17)	96(19)	89.71	89.96	89.86	0.05	970	935
DFS7	128(16)	66(16)	89.82	90.76	90.24	6.58	895	937
DFS8	103(16)	46(17)	89.94	91.40	90.47	1.26	929	934
DFS9	96(9)	56(17)	90.07	92.91	90.79	3.51	894	927
DFS10	155(17)	109(16)	89.93	91.15	90.64	0.36	1028	938
DFS11	238(18)	137(17)	89.18	90.43	89.84	0.41	1012	943
DFS13	113(17)	65(16)	89.91	91.90	91.15	1.14	946	914
DFS14	162(17)	108(17)	89.95	90.76	90.74	1.10	1031	937
DFS15	71(11)	36(15)	91.37	94.49	92.19	11.57	822	874
DFS16	141(17)	70(16)	90.00	91.11	90.84	2.15	1025	960

Note: Mg[#] is calculated by $Mg^{\#}=100 \times Mg/(Mg+Fe)$ in mol. “DFS” is the abbreviation of Dongfushan, which is the name of the volcano. Numbers in brackets are the number of grains that are used to calculate water concentration. All data in this table are from Hao et al., 2016. The two-pyroxenes geothermometer is from Brey et al. (1990) and the equilibrium pressure was assumed to be 15 kbar. (La/Yb)_n is primitive mantle normalized.

Table DR5. Contrasted OH absorbance in the core and rim of opx grains from the Tianchang peridotites.

Sample	Grain	Absorbance (cm ⁻²)		Sample	Grain	Absorbance (cm ⁻²)	
		Core	Rim			Core	Rim
DFS1	a	58.95	49.73	DFS9	a	35.97	23.72
	b	63.72	48.94		b	35.82	27.33
DFS2	a	53.91	41.74	DFS10	a	68.63	42.38
	b	63.85	32.48		b	72.51	48.03
DFS3	a	79.66	48.36	DFS11	a	64.45	52.50
	b	69.33	57.43		b	78.01	46.83
DFS4	a	57.63	44.57	DFS13	a	46.24	33.12
	b	53.31	38.00		b	38.97	25.91
DFS5	a	30.80	27.92	DFS14	a	63.87	50.73
	b	35.78	29.62		b	75.34	48.31
DFS6	a	43.61	35.69	DFS15	a	24.17	19.23
	b	50.21	36.36		b	22.91	18.57
DFS7	a	26.79	21.18	DFS16	a	32.69	17.51
	b	32.88	28.38		b	34.89	28.17
DFS8	a	42.15	27.78				
	b	34.93	30.50				

Note: a,b refer to two different opx grains. Absorbance is the integrated area of unpolarized FTIR spectrum, which is thickness-normalized.

Table DR6. The measured water content profile for DFS opx and their 1D or 3D modeling results.

References

- Bell, D. R., Ihinger, P. D., and Rossman, G. R., 1995, Quantitative-Analysis of Trace Oh in Garnet and Pyroxenes: *American Mineralogist*, v. 80, no. 5-6, p. 465-474.
- Bonadiman, C., Hao, Y., Coltorti, M., Dallai, L., Faccini, B., Huang, Y., & Xia, Q. (2009). Water contents of pyroxenes in intraplate lithospheric mantle. *European Journal of Mineralogy*, 21(3), 637-647.
- Brey, G. P., & Köhler, T. (1990). Geothermobarometry in four-phase lherzolites II. New thermobarometers, and practical assessment of existing thermobarometers. *Journal of Petrology*, 31(6), 1353-1378.
- Coogan, L. A., Hain, A., Stahl, S., & Chakraborty, S. (2005). Experimental determination of the diffusion coefficient for calcium in olivine between 900°C and 1500°C. *Geochimica et Cosmochimica Acta*, v. 69, p. 3683-3694.
- Crank, J., 1956, *The mathematics of diffusion*: Oxford.
- Demouchy, S., & Bolfan-Casanova, N. (2016). Distribution and transport of hydrogen in the lithospheric mantle: A review. *Lithos*, 240, 402-425.
- Dohmen, R., & Chakraborty, S. (2007). Fe–Mg diffusion in olivine II: point defect chemistry, change of diffusion mechanisms and a model for calculation of diffusion coefficients in natural olivine. *Physics and Chemistry of Minerals*, v. 34, p. 409-430.
- Hao, Y. T., Xia, Q. K., Tian, Z. Z., and Liu, J., 2016, Partial melting control of water contents in metasomatized lithospheric mantle: evidence from the Tianchang peridotite xenoliths of eastern China: *Lithos*, 260, 315-327.
- Niu, Y. L. (2005). Generation and evolution of basaltic magmas: some basic concepts and a new view on the origin of Mesozoic–Cenozoic basaltic volcanism in eastern China. *Geological Journal of China Universities*, 11(1), 9-46.
- Peck, D. L. (1978). *Cooling and vesiculation of Alae lava lake, Hawaii (No. 935-B)*. US Govt. Print. Off.
- Peslier, A. H. (2010). A review of water contents of nominally anhydrous natural minerals in the mantles of Earth, Mars and the Moon. *Journal of Volcanology and Geothermal Research*, 197(1), 239-258.

- Stalder, R., & Skogby, H. (2003). Hydrogen diffusion in natural and synthetic orthopyroxene. *Physics and Chemistry of Minerals*, 30(1), 12-19.
- Stalder, R., & Skogby, H. (2007). Dehydration mechanisms in synthetic Fe-bearing enstatite. *European journal of mineralogy*, 19(2), 201-216.
- Sundvall, R., Skogby, H., and Stalder, R., 2009a, Dehydration-hydration mechanisms in synthetic Fe-poor diopside: *European Journal of Mineralogy*, v. 21, no. 1, p. 17-26.
- Sundvall, R., Skogby, H., and Stalder, R., 2009b, Hydrogen diffusion in synthetic Fe-free diopside: *European Journal of Mineralogy*, v. 21, no. 5, p. 963-970.
- Xia, Q. K., Hao, Y., Li, P., Deloule, E., Coltorti, M., Dallai, L. & Feng, M. (2010). Low water content of the Cenozoic lithospheric mantle beneath the eastern part of the North China Craton. *Journal of Geophysical Research: Solid Earth*, 115(B7).
- Zou, H., Zindler, A., Xu, X., & Qi, Q. (2000). Major, trace element, and Nd, Sr and Pb isotope studies of Cenozoic basalts in SE China: mantle sources, regional variations, and tectonic significance. *Chemical Geology*, 171(1), 33-47.